Available online at www.sciencedirect.com

SCIENCE DIRECT®

Physics Letters B 632 (2006) 638–643

PHYSICS LETTERS B

www.elsevier.com/locate/physletb

Microscopic calculations of spin polarized neutron matter at finite temperature

I. Bombaci [a], A. Polls [b], A. Ramos [b], A. Rios [b], I. Vidaña [c,*]

[a] *Dipartimento di Fisica "E. Fermi" Università di Pisa and INFN Sezione di Pisa, Largo Bruno Pontecorvo 3, I-56127 Pisa, Italy*
[b] *Departament d'Estructura i Constituents de la Matèria, Universitat de Barcelona, Diagonal 647, E-08028 Barcelona, Spain*
[c] *Gesellschaft für Schwerionenforschung (GSI), Planckstrasse 1, D-64291 Darmstadt, Germany*

Received 21 June 2005; accepted 26 August 2005

Available online 18 November 2005

Editor: J.-P. Blaizot

Abstract

The properties of spin polarized neutron matter are studied both at zero and finite temperature within the framework of the Brueckner–Hartree–Fock formalism, using the Argonne v18 nucleon–nucleon interaction. The free energy, energy and entropy per particle are calculated for several values of the spin polarization, densities and temperatures together with the magnetic susceptibility of the system. The results show no indication of a ferromagnetic transition at any density and temperature.

PACS: 26.60.+c; 21.60.Jz; 26.50.+x

Keywords: Neutron matter; Ferromagnetic transition; Finite temperature

Since the suggestion of Pacini [1] and Gold [2] pulsars are generally believed to be rapidly rotating neutron stars with strong surface magnetic fields in the range of 10^{12}–10^{13} Gauss. Despite the great theoretical effort of the last forty years, there is still no general consensus regarding the mechanism to generate such strong magnetic fields in a neutron star. The fields could be a fossil remnant from that of the progenitor star or, alternatively, they could be generated after the formation of the neutron star by some long-lived electric currents flowing in the highly conductive neutron star material. From the nuclear physics point of view, however, one of the most interesting and stimulating mechanisms which have been suggested is the possible existence of a phase transition to a ferromagnetic state at densities corresponding to the theoretically stable neutron stars and, therefore, of a ferromagnetic core in the liquid interior of such compact objects. Such a possibility has been considered since long ago by several authors within different theoretical approaches [3–24], but the results are still contradictory. Whereas some calculations, like, for instance, the ones based on Skyrme-like interactions predict the transition to occur at densities in the range $(1–4)\rho_0$ ($\rho_0 = 0.16$ fm^{-3}), others, like recent Monte Carlo [20] and Brueckner–Hartree–Fock calculations [21–23] using modern two- and three-body realistic interactions exclude such a transition, at least up to densities around five times ρ_0. This transition could have important consequences for the evolution of a protoneutron star, in particular, for the spin correlations in the medium which do strongly affect the neutrino cross sections and the neutrino mean free path inside the star [25]. Therefore, drastically different scenarios for the evolution of protoneutron stars emerge depending on the existence of such a ferromagnetic transition.

Most of the studies of the ferromagnetic transition in neutron and nuclear matter have been done at zero temperature. However, the description of protoneutron stars [26] motivates a study of spin polarized neutron matter at temperature T of the order of a few tens of MeV. Recently, the properties of polarized neutron matter both at finite and zero temperature, have been investigated [27] using a large sample of Skyrme-like in-

* Corresponding author. Tel.: +49 6159 71 2754.
E-mail address: i.vidana@gsi.de (I. Vidaña).

0370-2693
doi:10.1016/j.physletb.2005.08.136

teractions. The results of Ref. [27] indicate the occurrence of a ferromagnetic phase of neutron matter. However, contrary to what one would intuitively expect, the authors of Ref. [27] have found that the critical density at which ferromagnetism takes place decreases with temperature. This unexpected result was associated to an anomalous behaviour of the entropy of the system which becomes larger for the spin-polarized phase with respect to the one for the non-polarized phase, above a certain density. This was shown to be related to the dependence of the effective masses of neutrons with spin up and down on the amount of spin-polarization, and a new constraint on the parameters of the Skyrme force was derived if this anomalous behaviour is to be avoided [27].

In the present work, we study the bulk and single particle properties of spin-polarized neutron matter at finite temperature. To this aim we make use of a microscopic approach based on the Brueckner–Hartree–Fock (BHF) approximation of the Brueckner–Bethe–Goldstone (BBG) expansion. Here we make use of an extension of the BBG theory (i) to the case in which neutron matter is arbitrarily asymmetric in the spin degree of freedom [21] (i.e., $\rho_\uparrow \neq \rho_\downarrow$, where $\rho_\uparrow$ ($\rho_\downarrow$) is the density of neutron with spin up (down)), and (ii) to the case of finite temperature. In particular, we study the behaviour of the entropy of the system and the effective mass of neutrons as a function of the spin polarization parameter, $\Delta = (\rho_\uparrow - \rho_\downarrow)/(\rho_\uparrow + \rho_\downarrow)$. We show that, contrary to what it is found in Ref. [27], the entropy of the polarized phase is lower than that of the non-polarized one, according to the idea that the polarized phase is more "ordered" than the non-polarized one.

Our calculation starts with the construction of the neutron-neutron G-matrix, which describes in an effective way the interaction between two neutrons for each one of the spin combinations $\uparrow\uparrow$, $\uparrow\downarrow$, $\downarrow\uparrow$ and $\downarrow\downarrow$. This is formally obtained by solving the well known Bethe–Goldstone equation, written schematically as

$$G(\omega)_{\sigma_1\sigma_2,\sigma_3\sigma_4} = V_{\sigma_1\sigma_2,\sigma_3\sigma_4} + \sum_{\sigma_i\sigma_j} V_{\sigma_1\sigma_2,\sigma_i\sigma_j} \frac{Q_{\sigma_i\sigma_j}}{\omega - \varepsilon_{\sigma_i} - \varepsilon_{\sigma_j} + i\eta} \times G(\omega)_{\sigma_i\sigma_j,\sigma_3\sigma_4}, \tag{1}$$

where the first (last) two subindices indicate the spin projection $\sigma = \uparrow(\downarrow)$ of the two neutrons in the initial (final) state, V is the bare nucleon–nucleon interaction, $Q_{\sigma_i\sigma_j}$ is the Pauli operator which allows only intermediate states compatible with the Pauli principle, and ω is the starting energy defined as the sum of the non-relativistic single-particle energies, $\varepsilon_{\uparrow(\downarrow)}$, of the interacting neutrons.

The single-particle energy of a neutron with momentum k and spin projection $\sigma = \uparrow(\downarrow)$ is given by

$$\varepsilon_\sigma(k) = \frac{\hbar^2 k^2}{2m} + \mathrm{Re}\big[U_\sigma(k)\big], \tag{2}$$

where the real part of the single-particle potential $U_\sigma(k)$ represents the averaged field "felt" by the neutron due to its interaction with the other neutrons of the system. In the BHF approximation it is given by

$$U_\sigma(k) = \sum_{\sigma' k'} n_{\sigma'}(k') \langle \vec{k}\sigma \vec{k}'\sigma' | G\big(\omega = \varepsilon_\sigma(k) + \varepsilon_{\sigma'}(k')\big) | \vec{k}\sigma\vec{k}'\sigma' \rangle_A \tag{3}$$

where

$$n_\sigma(k) = \begin{cases} 1, & \text{if } k \leqslant k_F^\sigma, \\ 0, & \text{otherwise,} \end{cases} \tag{4}$$

is the corresponding occupation number of a neutron with spin projection σ and the matrix elements are properly antisymmetrized. We note here that the so-called continuous prescription has been adopted for the single-particle potential when solving the Bethe–Goldstone equation. As shown by the authors of Refs. [28,29], the contribution to the energy per particle from three-body clusters is diminished in this prescription with respect to the one calculated with the gap choice for the single particle potential. We also note that the present calculation has been carried out using the Argonne v18 nucleon–nucleon potential [30]. The momentum dependence of the single-particle spectrum can be characterized by the effective mass $m^*_\sigma(k)$ defined as:

$$\frac{m^*_\sigma(k)}{m} = \frac{k}{m}\left(\frac{d\varepsilon_\sigma(k)}{dk}\right)^{-1}, \tag{5}$$

where m is the bare neutron mass.

The total energy per particle is easily obtained once a self-consistent solution of Eqs. (1)–(3) is achieved

$$\frac{E}{A} = \frac{1}{A}\sum_{\sigma k} n_\sigma(k)\left(\frac{\hbar^2 k^2}{2m} + \frac{1}{2}\,\mathrm{Re}\big[U_\sigma(k)\big]\right). \tag{6}$$

The many-body problem at finite temperature has been considered by several authors within different approaches, such as the finite temperature Green's function method [31], the thermo field method [32], or the Bloch–De Domicis (BD) diagrammatic expansion [33]. The latter, developed soon after the Brueckner theory, represents the "natural" extension to finite temperature of the BBG expansion, to which it leads in the zero temperature limit. Baldo and Ferreira [34] showed that the dominant terms in the BD expansion were those that correspond to the zero temperature of the BBG diagrams, where the temperature is introduced only through the Fermi–Dirac distribution

$$f_\sigma(k,T) = \frac{1}{1 + \exp([\varepsilon_\sigma(k,T) - \mu_\sigma(T)]/T)}, \tag{7}$$

$\mu_\sigma(T)$ being the chemical potential of a neutron with spin projection σ. Therefore, at the BHF level, finite temperature effects can be introduced in a very good approximation just replacing in the Bethe–Goldstone equation: (i) the zero temperature Pauli operator $Q_{\sigma_i\sigma_j} = (1 - n_{\sigma_i})(1 - n_{\sigma_j})$ by the corresponding finite temperature one $Q_{\sigma_i\sigma_j}(T) = (1 - f_{\sigma_i})(1 - f_{\sigma_j})$, and (ii) the single-particle energies $\varepsilon_\sigma(k)$ by the temperature dependent ones $\varepsilon_\sigma(k,T)$ obtained from Eqs. (2) and (3) when $n_\sigma(k)$ is replaced by $f_\sigma(k,T)$. These approximations, which are supposed to be valid in the range of densities and temperatures considered here, correspond to the "naive" finite temperature Brueckner–Bethe–Goldstone (NTBBG) expansion discussed in Ref. [34].

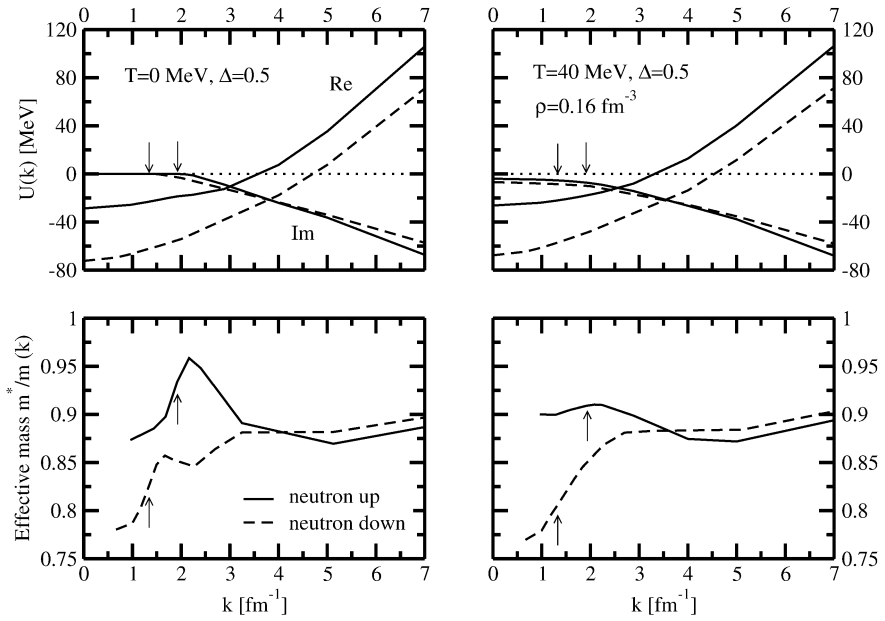

Fig. 1. Single-particle potential (top panels) and effective mass (bottom panels) of neutrons with spin up (solid lines) and spin down (dashed lines) as functions of the linear momentum at fixed density ($\rho = 0.16$ fm^{-3}) and spin polarization ($\Delta = 0.5$) for $T = 0$ (left panels) and $T = 40$ MeV (right panels). The arrows denote the value of the corresponding Fermi momenta.

In this case, however, the self-consistent process implies that, together with the Bethe–Goldstone equation and the single-particle potential, the chemical potentials of neutrons with spin up and down must be extracted at each step of the iterative process from the normalization condition

$$\rho_\sigma = \sum_k f_\sigma(k,T). \tag{8}$$

This is an implicit equation which can be solved numerically. Note that the G-matrix obtained from the Bethe–Goldstone equation (1) and also the single-particle potentials depend implicitly on the chemical potentials.

Once a self-consistent solution is achieved the total free energy per particle is determined by

$$\frac{F}{A} = \frac{E}{A} - T\frac{S}{A}, \tag{9}$$

where E/A is evaluated from Eq. (6) replacing $n_\sigma(k)$ by $f_\sigma(k,T)$ and the total entropy per particle, S/A, is calculated through the expression

$$\frac{S}{A} = -\frac{1}{A}\sum_{\sigma k}\big[f_\sigma(k,T)\ln\big(f_\sigma(k,T)\big) + \big(1-f_\sigma(k,T)\big)\ln\big(1-f_\sigma(k,T)\big)\big]. \tag{10}$$

From the free energy per particle, we can get the remaining macroscopic properties of the system. In our case, we are particularly interested in the magnetic susceptibility χ, which characterizes the response of a system to a magnetic field and gives a measure of the energy required to produce a net spin alignment in the direction of the field. It is given by

$$\chi = \frac{\mu^2\rho}{(\frac{\partial^2(F/A)}{\partial\Delta^2})_{\Delta=0}}, \tag{11}$$

where μ is the magnetic moment of the neutron.

The single-particle potentials of neutrons with spin up and down have been simultaneously and self-consistently calculated together with their effective interactions. The results at $\rho = 0.16$ fm^{-3} and spin polarization $\Delta = 0.5$ are reported for $T = 0$ (left panel) and $T = 40$ MeV (right panel) on the top panels of Fig. 1. The neutron single-particle potential splits up in two different components when a partial spin polarization is assumed. In the case of Fig. 1, the single-particle potential $\mathrm{Re}[U_\uparrow(k)]$ for neutrons with spin up (the most abundant component) is less attractive than the one for neutrons with spin down, $\mathrm{Re}[U_\downarrow(k)]$. As demonstrated by the authors of Ref. [22] (see, in particular, their Eqs. (23) and (24)), this splitting (i) is the result of a *phase space effect*, i.e., to the change in the number of pairs which the neutron under consideration $|k,\sigma\rangle$ can form with the remaining neutrons $|k \leqslant k_F^{\sigma'}, \sigma' = \uparrow,\downarrow\rangle$ of the system as neutron matter is polarized, and (ii) is due to the spin dependence of the neutron–neutron G-matrix in the spin polarized medium (see Eq. (1)). Indeed, as polarization increases, the single particle potential of a spin up neutron is built from a larger number of up–up pairs that form a spin triplet state ($S = 1$) and, due to the Pauli principle, can only interact through odd angular momentum partial waves. Conversely, the potential of the less abundant species is built from a relatively larger number of up–down pairs which can interact both in the $S = 0$ and $S = 1$ two body states. Thus, the potential of the less abundant species receives also contributions from some important attractive channels as, e.g., the $^1S_0$.

The increase of the temperature changes moderately the single-particle potentials. The real part becomes slightly less attractive, whereas the imaginary part increases in size as a consequence of the increase of phase space in the low momentum region.

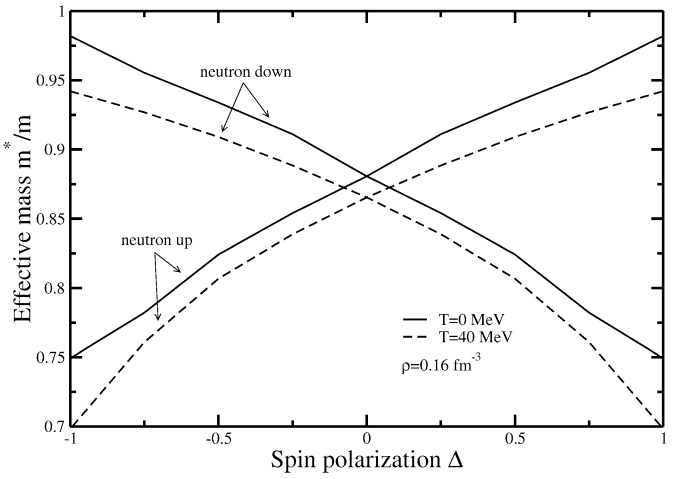

Fig. 2. Neutron effective mass at the corresponding Fermi surface of the spin up and down components as a function of the spin polarization at $\rho = 0.16$ fm^{-3} for $T = 0$ and $T = 40$ MeV.

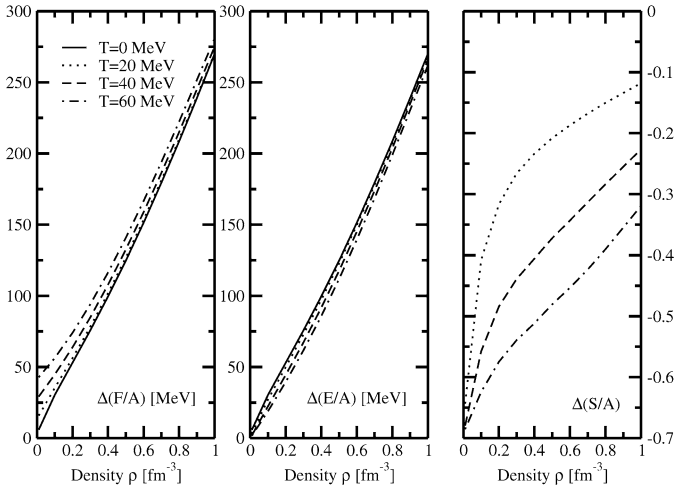

Fig. 3. Differences of the free energy (left panel), energy (central panel) and entropy per particle (right panel) between fully polarized and non-polarized neutron matter as a function of density for several temperatures.

The momentum dependence of the corresponding effective masses of the two components is also shown in the bottom panels of the figure for the same values of density, spin polarization and temperatures. The general effect of temperature is to smooth out the enhancement of the effective mass near the Fermi surface, as observed in the work of Ref. [35] in symmetric nuclear matter.

In Fig. 2 we show the effective mass $m^*_\uparrow(m^*_\downarrow)$ for neutrons with spin up (down) as a function of the spin polarization Δ, for fixed density ($\rho = 0.16$ fm^{-3}) and temperature ($T = 0$ and $T = 40$ MeV). The effective mass is calculated using Eq. (5) taken for each component at the corresponding Fermi momentum. Obviously, for $\Delta = 0$ the effective mass of the two components coincides. Once some amount of polarization is considered, the values of the effective masses split in two, the effective mass of the most abundant component being larger than the one of the less abundant. As can be seen the effective masses show an almost linear and symmetric variation with respect to their common value at spin polarization $\Delta = 0$, both at $T = 0$ and $T = 40$ MeV. Deviations from this behaviour are only found at the higher polarization values. This behaviour of m^*_σ is a direct consequence of the scissors-like dependence of the single particle potential Re$[U_\sigma]$ as a function of the spin polarization parameter Δ (see Fig. 2 of Ref. [22]). A similar qualitative behaviour for the nucleon effective mass, as a function of the isospin asymmetry parameter, $\beta = (\rho_n - \rho_p)/\rho$, has been found in isospin asymmetric nuclear matter [36–38] (see, in particular, Eq. (94) in Ref. [37]).

The differences of the free energy (F/A), energy (E/A) and entropy (S/A) per particle between the totally polarized and the non-polarized phases are reported in the left, central and right panels of Fig. 3 as a function of the density for several temperatures. The differences in the three quantities increase with density and increase (decrease) with temperature in the case of the free energy (energy and entropy). Contrary to the results of Ref. [27] with the Skyrme interaction, these differences are always positive for the F/A and E/A. This is an indication that the non-polarized phase is energetically preferred in the range

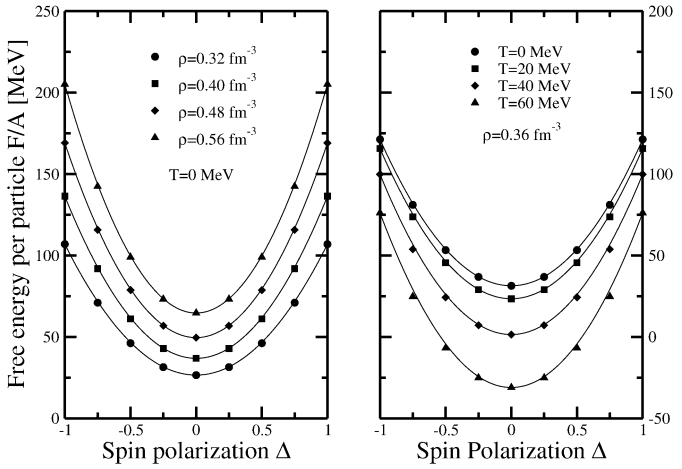

Fig. 4. Left panel: free energy per particle at zero temperature as a function of the spin polarization for several densities. Right panel: free energy per particle at a fixed density $\rho = 0.36$ fm^{-3} as a function of the spin polarization for several temperatures. Circles, squares, diamonds and triangles show our BHF results, whereas the solid lines correspond to the parabolic approximation defined in Eq. (12).

of densities explored. Therefore, we can conclude that a phase transition to a ferromagnetic state is not to be expected from our microscopic calculation. If such a transition would exist, the difference in the free energy would become zero at some density, indicating that the ground state of the system would be ferromagnetic from that density on. In addition, the difference in the entropy is always negative indicating, as one intuitively expects, that the totally polarized phase is more "ordered" than the non-polarized one.

In Fig. 4 we show the behaviour of the free energy F/A per particle as a function of the spin polarization for several densities (left panel) and temperatures (right panel). Circles, squares, diamonds and triangles correspond to our BHF results, whereas the solid lines correspond to the parabolic approximation discussed below. As we expected from our previous calculations at zero temperature [21] and [22], F/A is symmetric in Δ and

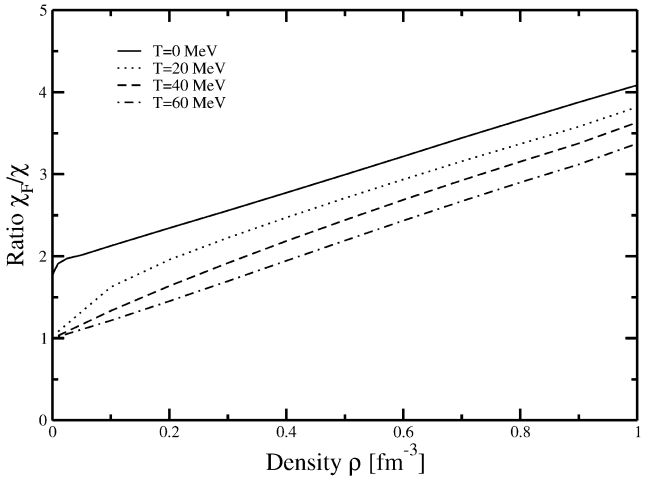

Fig. 5. Ratio between the magnetic susceptibility of the free Fermi gas and the corresponding magnetic susceptibility of interacting neutron matter as a function of density for several temperatures.

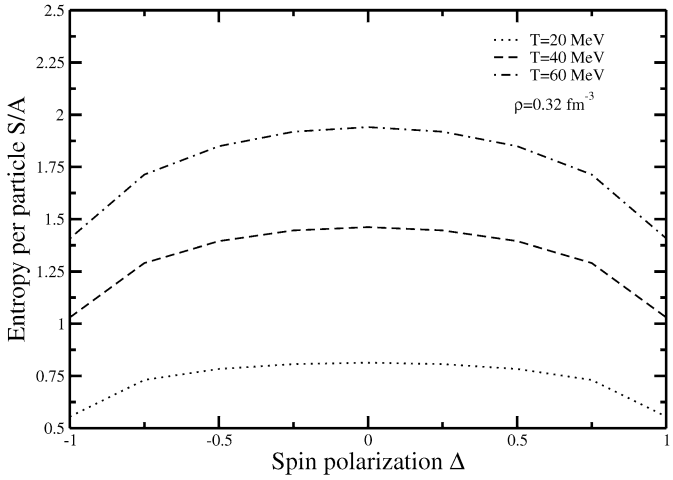

Fig. 6. Entropy per particle as a function of the spin polarization at $\rho = 0.32$ fm^{-3} for several temperatures.

it shows a minimum at $\Delta = 0$ for all the densities and temperatures considered. This is again an indication that the ground state of neutron matter is paramagnetic, in opposition to what it is found in Ref. [27] for Skyrme-like interactions where, as a consequence of the anomalous behaviour of the entropy, the minimum of F/A is situated at $0 < \Delta < 1$ and moves to higher polarizations when the temperature increases. It is also interesting to note that the dependence of F/A on the spin polarization is "up to a very good approximation" parabolic. One can try to characterize that dependence in the following simple analytic form:

$$\frac{F}{A}(\rho, \Delta, T) = \frac{F}{A}(\rho, 0, T) + a(\rho, T)\Delta^2 \tag{12}$$

where, assuming the quadratic dependence to be valid up to $|\Delta| = 1$ as our results indicate, the value of $a(\rho, T)$ can be easily obtained for each density and temperature as the difference between the total free energies per particle of totally polarized and non-polarized neutron matter

$$a(\rho, T) = \frac{F}{A}(\rho, \pm 1, T) - \frac{F}{A}(\rho, 0, T). \tag{13}$$

The magnetic susceptibility can be evaluated then in a very simple way if the parabolic dependence of Eq. (12) is assumed, giving

$$\chi(\rho, T) = \frac{\mu^2 \rho}{2a(\rho, T)}. \tag{14}$$

The ratio χ_F/χ, where χ_F is the magnetic susceptibility of the free Fermi gas, is shown in Fig. 5 as a function of density for several temperatures. Starting from 1, the ratio increases as the density increases at any temperature and no signal of a change of such a trend is expected at higher densities, contrary to the results of Ref. [27] in the case of the Skyrme-like interactions. This is again an indication that a ferromagnetic transition, whose onset would be signaled by the density at which this ratio becomes zero, is not seen and not expected at larger densities either.

Finally, the behaviour of the entropy per particle S/A as a function of the spin polarization at a fixed density $\rho = 0.32$ fm^{-3} for several temperatures is shown in Fig. 6. The entropy, as the free energy, is also symmetric and almost parabolic in Δ. Its maximum is placed at $\Delta = 0$ for all the densities and temperatures considered, as one naively expects, contrary to the findings of Ref. [27]. In this reference, it was shown that for a pure parabolic single particle spectrum, as it is the case for the Skyrme interaction, imposing the entropy of the polarized phase to be smaller than the unpolarized one for a given density and temperature, is equivalent to requiring the ratio of the neutron effective masses in the fully polarized and unpolarized phases to be smaller than $2^{2/3}$. In the BHF approach, the momentum and temperature dependence of the effective mass prevents from deriving a similar rigorous condition. However, thinking in terms of a value of the effective mass that would characterize the single particle spectrum in average, or considering just the effective mass at the Fermi surface, which is the most relevant for the calculation of the entropy at small temperatures, we can then explore if the BHF calculations respect the condition derived in [27]. In fact, in the case of $\rho = 0.16$ fm^{-3} and $T = 40$ MeV we find (see Fig. 2) $m^*_{\uparrow}(\Delta = 1)/m^*_{\uparrow(\downarrow)}(\Delta = 0) = 1.09$, which is smaller than the limit established in Ref. [27]. This is true for all the densities and temperatures explored in this work and therefore the entropy of the polarized phase is always smaller than that for the unpolarized one.

In summary, we have studied the properties of spin polarized neutron matter both at zero and finite temperature within the framework of the Brueckner–Hartree–Fock formalism. We have determined the single-particle potentials and the effective mass of neutrons with spin up and down for arbitrary values of the density, temperature and spin polarization. We have found that the spin up and spin down effective masses show an almost linear and symmetric variation with respect to their values at spin polarization $\Delta = 0$.

We have determined the differences of the free energy (F/A), energy (E/A) and entropy (S/A) per particle between the totally polarized and non-polarized phases. We have found

that, in contrast to the results of a similar study with the Skyrme interaction [27], these differences are always positive for the F/A and E/A which is an indication that the non-polarized phase is energetically favorable, from which we can conclude that a phase transition to a ferromagnetic state is not to be expected. In addition, contrary to the results with the Skyrme interaction, we have found that the difference in the entropy is always negative according to the idea that the totally polarized phase is more "ordered" than the non-polarized one.

Finally, we have seen that both the free energy and the entropy per particle are not only symmetric on the spin polarization but also parabolic in a very good approximation up to $|\Delta| = 1$. This finding supports the calculation of the magnetic susceptibility by using only the free energies of the fully polarized and non-polarized phases.

Acknowledgements

This work is partially supported by DGICYT (Spain) project BFM2002-01868 and by the Generalitat de Catalunya project 2001SGR00064. This research is part of the EU Integrated Infrastructure Initiative Hadron Physics project under contract number RII3-CT-2004-506078. One of the authors (A. Rios) acknowledges the support from DURSI and the European Social Funds.

References

[1] F. Pacini, Nature (London) 216 (1967) 567.
[2] T. Gold, Nature (London) 218 (1968) 731.
[3] D.H. Brownell, J. Callaway, Nuovo Cimento B 60 (1969) 169.
[4] M.J. Rice, Phys. Lett. A 29 (1969) 637.
[5] J.W. Clark, N.C. Chao, Lett. Nuovo Cimento 2 (1969) 185.
[6] J.W. Clark, Phys. Rev. Lett. 23 (1969) 1463.
[7] S.D. Silverstein, Phys. Rev. Lett. 23 (1969) 139.
[8] E. Østgaard, Nucl. Phys. A 154 (1970) 202.
[9] J.M. Pearson, G. Saunier, Phys. Rev. Lett. 24 (1970) 325.
[10] V.R. Pandharipande, V.K. Garde, J.K. Srivastava, Phys. Lett. B 38 (1972) 485.
[11] S.O. Bäckman, C.G. Källman, Phys. Lett. B 43 (1973) 263.
[12] P. Haensel, Phys. Rev. C 11 (1975) 1822.
[13] A.D. Jackson, E. Krotscheck, D.E. Meltzer, R.A. Smith, Nucl. Phys. A 386 (1982) 125.
[14] M. Kutschera, W. Wójcik, Phys. Lett. B 223 (1989) 11.
[15] S. Marcos, R. Niembro, M.L. Quelle, J. Navarro, Phys. Lett. B 271 (1991) 277.
[16] P. Bernardos, S. Marcos, R. Niembro, M.L. Quelle, Phys. Lett. B 356 (1995) 175.
[17] A. Vidaurre, J. Navarro, J. Bernabeu, Astron. Astrophys. 135 (1984) 361.
[18] J. Margueron, J. Navarro, N.V. Giai, Phys. Rev. C 66 (2002) 014303.
[19] M. Kutschera, W. Wójcik, Phys. Lett. B 325 (1994) 271.
[20] S. Fantoni, A. Sarsa, K.E. Schmidt, Phys. Rev. Lett. 87 (2001) 181101.
[21] I. Vidaña, A. Polls, A. Ramos, Phys. Rev. C 65 (2002) 035804.
[22] I. Vidaña, I. Bombaci, Phys. Rev. C 66 (2002) 045801.
[23] W. Zuo, U. Lombardo, C.W. Shen, in: W.M. Alberico, M. Nardi, M.P. Lombardo (Eds.), Quark–Gluon Plasma and Heavy Ion Collisions, World Scientific, Singapore, 2002, p. 192.
[24] A.A. Isayev, J. Yang, Phys. Rev. C 69 (2004) 025801.
[25] J. Navarro, E.S. Hernández, D. Vautherin, Phys. Rev. C 60 (1999) 045801.
[26] M. Prakash, I. Bombaci, M. Prakash, P.J. Ellis, J.M. Lattimer, R. Knorren, Phys. Rep. 280 (1997) 1.
[27] A. Rios, A. Polls, I. Vidaña, Phys. Rev. C 71 (2005) 055802.
[28] H.Q. Song, M. Baldo, G. Giansiracusa, U. Lombardo, Phys. Rev. Lett. 81 (1998) 1584.
[29] M. Baldo, G. Giansiracusa, U. Lombardo, H.Q. Song, Phys. Lett. B 473 (2000) 1.
[30] R.B. Wiringa, V.G.J. Stoks, R. Schiavilla, Phys. Rev. C 51 (1995) 38.
[31] A.L. Fetter, J.D. Walecka, Quantum Theory of Many Particle Physics, McGraw–Hill, New York, 1971.
[32] For a recent review see: P.A. Hening, Phys. Rep. 253 (1995) 235.
[33] C. Bloch, Nucl. Phys. 7 (1958) 451;
C. Bloch, C. De Domicis, Nucl. Phys. 7 (1958) 459;
C. Bloch, C. De Domicis, Nucl. Phys. 10 (1959) 181;
C. Bloch, C. De Domicis, Nucl. Phys. 10 (1959) 509.
[34] M. Baldo, L. Ferreira, Phys. Rev. C 59 (1999) 682.
[35] A. Lejeune, P. Grangé, M. Martzolff, J. Cugnon, Nucl. Phys. A 453 (1986) 189.
[36] I. Bombaci, U. Lombardo, Phys. Rev. C 44 (1991) 1892.
[37] I. Bombaci, in: M. Baldo (Ed.), Nuclear Methods and the Nuclear Equation of State, World Scientific, Singapore, 1999, p. 381.
[38] B.-A. Li, Phys. Rev. C 69 (2004) 064602.